

120  
4-22-92 85③

NIPER-573  
(DE92001035)

**DEVELOPMENT OF GENERAL INFLOW PERFORMANCE  
RELATIONSHIPS (IPR'S) FOR SLANTED AND HORIZONTAL  
WELLS PRODUCING HETEROGENEOUS SOLUTION-GAS  
DRIVE RESERVOIRS**

By  
**Aaron M. Cheng**

**April 1992**

**Performed Under Cooperative Agreement No. DE-FC22-83FE60149**

**IIT Research Institute  
National Institute for Petroleum and Energy Research  
Bartlesville, Oklahoma**

---

**Bartlesville Project Office  
U. S. DEPARTMENT OF ENERGY  
Bartlesville, Oklahoma**

## **DISCLAIMER**

**This report was prepared as an account of work sponsored by an agency of the United States Government. Neither the United States Government nor any agency thereof, nor any of their employees, makes any warranty, express or implied, or assumes any legal liability or responsibility for the accuracy, completeness, or usefulness of any information, apparatus, product, or process disclosed, or represents that its use would not infringe privately owned rights. Reference herein to any specific commercial product, process, or service by trade name, trademark, manufacturer, or otherwise does not necessarily constitute or imply its endorsement, recommendation, or favoring by the United States Government or any agency thereof. The views and opinions of authors expressed herein do not necessarily state or reflect those of the United States Government or any agency thereof.**

**This report has been reproduced directly from the best available copy.**

**Available to DOE and DOE contractors from the Office of Scientific and Technical Information, P.O. Box 62, Oak Ridge, TN 37831; prices available from (615)576-8401, FTS 626-8401.**

**Available to the public from the National Technical Information Service, U.S. Department of Commerce, 5285 Port Royal Rd., Springfield, VA 22161.**

NIPER--573

DE92 001035

NIPER-573

Distribution Category UC-122

DEVELOPMENT OF GENERAL INFLOW PERFORMANCE  
RELATIONSHIPS (IPR'S) FOR SLANTED AND HORIZONTAL WELLS  
PRODUCING HETEROGENEOUS SOLUTION-GAS DRIVE RESERVOIRS

By  
Aaron M. Cheng

April 1992

Work Performed Under Cooperative Agreement No. DE-FC22-83FE60149

Prepared for  
U.S. Department of Energy  
Assistant Secretary for Fossil Energy

Thomas B. Reid, Project Manager  
Bartlesville Project Office  
P. O. Box 1398  
Bartlesville, OK 74005

Prepared by  
IIT Research Institute  
National Institute for Petroleum and Energy Research  
P. O. Box 2128  
Bartlesville, OK 74005

MASTER

JP

## TABLE OF CONTENTS

	<u>Page</u>
Abstract.....	1
Introduction.....	1
Acknowledgments .....	1
Literature Review .....	1
Assumptions.....	2
Procedures for Generating IPR Data .....	2
Selection of Grid Data and Time Step Size.....	2
General Physical Interpretation of IPR Curves .....	5
Comparison of Pressure and Gas Saturation Profiles for Vertical and Horizontal Wells .....	6
IPR Results of Horizontal and Slanted Wells.....	6
Horizontal well IPR.....	6
Base Case .....	6
Vertical Permeability.....	7
Eccentricity.....	7
Stratification .....	7
Perforated Length .....	7
Formation Thickness .....	7
Heterogeneous Permeability .....	7
Slanted Well IPR .....	8
85.68 Degree - Slanted well.....	8
Base Case .....	8
Vertical Permeability .....	8
Eccentricity .....	8
Stratification .....	8
Perforated Length .....	8
Formation Thickness .....	9
Heterogeneous Permeability .....	9
75 Degree - Slanted Well .....	9
Base Case .....	9
Vertical Permeability .....	9
Eccentricity .....	9
Stratification .....	9
Perforated Length .....	10

## TABLE OF CONTENTS -- Continued

	<u>Page</u>
Formation Thickness .....	10
Heterogeneous Permeability .....	10
IPR Data Interpolation and Software .....	10
Results and Conclusions .....	10
References .....	10
Appendix A - User's Manual for Inflow Performance Relationship (IPR) Generator .....	21
Appendix B - Description of IPR Generator Help Command .....	26

## TABLES

1. Base data (based on case 1 of Vogel) .....	2
2. Reservoir grid block dimensions shown in figure 1 .....	3

## ILLUSTRATIONS

1. 19 x 3 x 3 Reservoir grid and well orientation for horizontal and slanted wells .....	4
2. Reservoir pressure vs. cumulative oil production, Np/N .....	12
3. Oil flow rate vs. cumulative oil production, Np/N .....	12
4. Gas-oil ratio (GOR) vs. cumulative oil production, Np/N .....	12
5. Reservoir pressure along x-direction from wellbore. Horizontal vs. vertical well .....	12
6. Reservoir gas saturation along x-direction distance from wellbore. Horizontal vs. vertical well. pwf = 100 psia .....	13
7. Reservoir pressure along x-direction distance from wellbore. Horizontal vs. vertical well. pwf = 600 psia .....	13
8. Reservoir gas saturation along x-direction distance from wellbore. Horizontal vs. vertical well. pwf = 600 psia .....	13
9. Inflow performance relationship (IPR) curves for horizontal and vertical well at 0.1% oil depletion .....	13
10. Horizontal well inflow performance relationship; base case .....	14
11. Horizontal well inflow performance relationship; vertical permeability = 0.1 x horizontal permeability .....	14
12. Horizontal well inflow performance relationship; wellbore in bottom layer of 19 x 3 x 3 grid .....	14
13. Horizontal well inflow performance relationship; wellbore in top layer of 19 x 3 x 3 grid .....	14
14. Horizontal well inflow performance relationship; strata permeability = 40, 20, 10 mD (top, middle, and bottom) .....	15
15. Horizontal well inflow performance relationship; strata permeability = 10, 20, 40 mD (top, middle, and bottom) .....	15
16. Horizontal well inflow performance relationship; perforated length = 1/3 x total well length .....	15

17. Horizontal well inflow performance relationship; formation thickness = 235 ft = 10 x base case .....	15
18. Horizontal well inflow performance relationship; heterogeneous permeability, permeability decreases from left to right by 20%.....	16
19. 85.68-Deg Slanted well inflow performance relationship; base case .....	16
20. 85.68-Deg Slanted well inflow performance relationship; vertical permeability = 0.1 x horizontal permeability .....	16
21. 85.68-Deg Slanted well inflow performance relationship; wellbore in bottom layer of 19 x 3 x 3 grid .....	16
22. 85.68-Deg Slanted well inflow performance relationship; wellbore in top layer of 19 x 3 x 3 grid.....	17
23. 85.68-Deg Slanted well inflow performance relationship; strata permeability = 40, 20, 10 mD (top, middle, and bottom).....	17
24. 85.68-Deg Slanted well inflow performance relationship; strata permeability = 10, 20, 40 mD (top, middle, and bottom).....	17
25. 85.68-Deg Slanted well inflow performance relationship; perforated length = 1/3 x total well length .....	17
26. 85.68-Deg Slanted well inflow performance relationship; formation thickness = 235 ft = 10 x base case .....	18
27. 85.68-Deg Slanted well inflow performance relationship; heterogeneous permeability, permeability decreases from left to right by 20%.....	18
28. 75-Deg Slanted well inflow performance relationship; base case .....	18
29. 75-Deg Slanted well inflow performance relationship; vertical permeability = 0.1 x horizontal permeability .....	18
30. 75-Deg Slanted well inflow performance relationship; wellbore in bottom layer of 19 x 3 x 3 grid.....	19
31. 75-Deg Slanted well inflow performance relationship; wellbore in top layer of 19 x 3 x 3 grid.....	19
32. 75-Deg Slanted well inflow performance relationship; strata permeability = 40, 20, 10 mD (top, middle, and bottom).....	19
33. 75-Deg Slanted well inflow performance relationship; strata permeability = 10, 20, 40 mD (top, middle, and bottom).....	19
34. 75-Deg Slanted well inflow performance relationship; perforated length = 1/3 total well length .....	20
35. 75-Deg Slanted well inflow performance relationship; formation thickness = 235 ft = 10 x base case.....	20
36. 75-Deg Slanted well inflow performance relationship; heterogeneous permeability, permeability decreases from left to right by 20%.....	20

# Development of General Inflow Performance Relationships (IPRs) for Slanted and Horizontal Wells Producing From Heterogeneous Solution-Gas Drive Reservoirs

By Aaron M. Cheng

## Abstract

Since 1968, the Vogel equation has been used extensively and successfully for analyzing the inflow performance relationship (IPR) of flowing vertical wells producing by solution-gas drive. Oil well productivity can be rapidly estimated by using the Vogel IPR curve and well outflow performance. With recent interests on horizontal well technology, several empirical IPRs for solution-gas drive horizontal and slanted wells have been developed under homogeneous reservoir conditions. This report presents the development of IPRs for horizontal and slanted wells by using a special vertical/horizontal/slanted well reservoir simulator under six different reservoir and well parameters: ratio of vertical to horizontal permeability, wellbore eccentricity, stratification, perforated length, formation thickness, and heterogeneous permeability. The pressure and gas saturation distributions around the wellbore are examined. The fundamental physical behavior of inflow performance for horizontal wells is described.

## Introduction

With recent technological advances in horizontal well drilling, horizontal well technology has quickly emerged as a promising method to boost well productivity and reserves. Additionally, the horizontal well technology can be used as an alternative or supplement to enhanced oil recovery (EOR) processes and infill drilling. In certain geologic conditions such as thin-pay and naturally fractured systems, this new technology can be the only means to produce hydrocarbons commercially. Likewise, it can provide more comprehensive reservoir descriptions than were previously possible. At the 1989 International Symposium on EOR in Maracaibo, Venezuela, it was concluded that horizontal well drilling (and steam injection) will play major roles in the future of EOR.

With declines in domestic reserves and gradual increases in imported oil, horizontal well drilling currently appears to be the most cost-effective method for adding petroleum reserves to new and existing fields and marginal fields near abandonment in the United States.

To decide whether to drill a conventional vertical or a horizontal well, the type of well that will result in the highest productivity and economic return must be selected. Common practice in the oil industry for making this selection is to calculate well productivity by using the well inflow performance relationship (IPR). Simply stated, an IPR describes the relationship of well flowing bottomhole pressure  $p_{wf}$  versus oil flow rate  $q_o$  at a stabilized reservoir pressure. For quick and accurate generation of the IPR

curve, use of the empirical Vogel<sup>1</sup> equation, developed in 1968, has been the most frequently used technique in the oil industry; however, the Vogel equation or curve is valid only for vertical wells. Recently, with DOE funding, NIPER has developed IPRs for slanted and horizontal wells<sup>2-3</sup> by using a special vertical/horizontal/slanted well reservoir simulator (hereafter called horizontal well simulator).<sup>4-5</sup> These IPRs represent wells producing from homogeneous and isotropic reservoir systems under the solution-gas drive producing mechanism. Since most reservoirs are heterogeneous, there is a need to develop and understand horizontal IPRs for heterogeneous systems.

This project has two main objectives: (1) to adapt the NIPER horizontal well reservoir simulator for an IBM PC/AT type microcomputer and (2) to develop IPRs for slanted and horizontal wells producing from heterogeneous solution-gas reservoir systems using the NIPER simulator. Objective (1) has been achieved; the PC version of the horizontal well simulator was completed and submitted to DOE in July, 1991.<sup>5</sup> This report presents the results of objective 2. Six reservoir and well parameters were selected to study their influence on well inflow performance: vertical permeability, wellbore eccentricity, stratification, perforated length, formation thickness, and heterogeneous permeability. In particular, pressure and gas saturation profiles, oil flow rates, gas-oil ratios (GOR), and reservoir pressures for the base case data of the horizontal and slanted wells were examined to understand better the physical phenomenon of the inflow behavior of these wells.

## Acknowledgments

This project was conducted for the U. S. Department of Energy under Cooperative Agreement DE-FC22-83FE60149. Special thanks are due to Fred Burch and Thomas Reid of the DOE Bartlesville Project Office for their initiation and supervision of this project, and to Thomas E. Burchfield, Ming-Ming Chang, James F. Pautz, Michael P. Madden and Min K. Tham, all of NIPER, for their valuable ideas and technical support.

## Literature Review

Recently Norris et al.<sup>5</sup> presented a comprehensive review of predicting horizontal well performance. It contains 84 references. IPRs of horizontal and slanted wells have been developed for single-phase (oil) flow. Most of these equations are analytical in nature and require properties such as formation permeability to compute well productivity. However, regarding two-phase (oil and gas) inflow performance relationship (IPR) for solution-gas

drive horizontal wells, only three references were quoted.<sup>7-8</sup> The two most significant studies on empirical two-phase IPR's of horizontal wells are those of Bendakhli and Aziz<sup>7</sup> and Cheng.<sup>3</sup> Both IPR generations were obtained by reservoir simulators. Empirical two-phase IPRs for slanted wells have been reported.<sup>2-3</sup>

### Assumptions

The major assumptions for generating horizontal and slanted well IPR data are similar to the ones previously presented.<sup>2</sup> For the base case of a horizontal well, they include the following. The well is located in the center of a completely bounded reservoir of rectangular prism geometry. The reservoir is homogeneous and isotropic with a constant water saturation. Thus permeability and porosity in the x, y, and z directions are equal. Water saturation is immobile during depletion of the well. Therefore, only two-phase flow, oil and gas, is considered in the reservoir. The well is producing under a semisteady state condition. Capillary pressure forces of reservoir fluids are neglected. The assumptions for the base case of a slanted well are similar. In this project, the IPRs for horizontal and slanted wells were generated by inputting various reservoir and well parameters mentioned previously; they were compared with those of the base case.

### Procedures for Generating IPR Data

There are several ways to deplete a solution-gas drive reservoir and obtain IPR data using a reservoir simulator: constant rate control, constant pressure control, constant rate control followed by pressure control, and constant pressure control followed by constant rate control. Bendakhli and Aziz<sup>7</sup> have reported that they obtained better resolution runs using the constant pressure control option than the constant rate option in their simulation runs. After several trial runs in this study, it also appeared that using the pressure control option in executing the NIPER horizontal well reservoir simulator gave the most stable results and that option was selected as the method to deplete the reservoir and generate IPR data. The procedures for generating the IPR data under the constant pressure control option are as follows.

1. At a predetermined flowing bottomhole pressure, e. g.,  $p_{wf} = 14.7$  psia, run the horizontal well depletion to a certain time such that at least 10% of the original oil in place (OOIP) is produced or depleted, if the input data permit to do so. (In some runs when  $p_{wf}$  is high, e. g.,  $p_{wf} = 1,800$  psia, the reservoir can deplete no more than 4% OOIP.)
2. At each of the cumulative oil production  $N_p/N$ , of 0.1, 2, 4, 6, 8, 10%, record the corresponding oil flow rate, gas flow rate, oil and gas cumulative production, and reservoir pressure.

3. To normalize the IPR data, compute  $p' = p_{wf}/p_r$  and  $q' = q_{oil}/q_{omax}$  to obtain an IPR plot; plot  $p'$  vs.  $q'$  on a normal scale with  $p'$  on the y axis and  $q'$  on the x axis.

4. Repeat the above three steps for a different flowing bottomhole pressure; the IPR data in this study were generated at  $p_{wf} = 14.7, 100, 200, 300, 400, 450, 500, 600, 800, 1,000, 1,200, 1,400, 1,600$  and  $1,800$  psia.

Because of the unstable IPR results obtained in certain circumstances discussed later, sometimes it may be necessary to examine a range of flow data at a given  $N_p/N$  value and decide the best IPR point at that  $N_p/N$  and  $p_{wf}$ . However, when a small fixed time step of 0.01 day was used to generate the IPR data, the flow results appeared to be stable and the corresponding  $p_{wf}$ ,  $q_o$ , and  $p_r$  were recorded at a given  $N_p/N$  to generate the normalized IPR curve.

### Selection of Grid Data and Time Step Size

The base case reservoir data of Vogel<sup>1</sup> were selected as the principal reservoir data for generating IPR results for horizontal and slanted wells. These data include basic reservoir data (Table 1), fluid PVT, and oil-gas relative permeability data.<sup>1</sup>

At the beginning (July 1990) of this project, it was expected that a large number of simulation runs ( $>10,000$ ) would be required to generate IPR data for horizontal and slanted wells producing from heterogeneous systems. At that time, the available computer system was an 8 MB microVAX -II with a 0.9 Vax Processing Units (VPU) speed (1 VPU is approximately equal to 1 million instructions per second, MIPS). It was determined that the execution of hundreds of simulation runs with more than 150 grid blocks involving fine grid computations would not be feasible on the computer system. Thus the selection of an appropriate simulation grid size that could generate reliable results in minimal computer time was very important.

TABLE 1  
Base Data (Based on Case 1 of Vogel)<sup>1</sup>

Initial reservoir pressure, psia	2144.7
Bubble point pressure, psia	2144.7
Reservoir drainage area, acres	20
Well radius, ft	0.33
Net pay, ft	23.5
Porosity, %	13.9
Permeability, mD	20
Initial water saturation, %	19.4
Critical gas saturation, %	2.1
Oil gravity, °API	40
Gas specific gravity	0.8
Formation compressibility, $\text{psi}^{-1}$	$4.2 \times 10^{-6}$

During the early phase of this project, the  $5 \times 5 \times 3$  grid previously used in generation of IPR data for homogeneous systems was selected for generation of initial IPRs for this project. However, initial IPR results generated using this coarse grid appeared to be inappropriate. The  $5 \times 3 \times 3$  grid was not fine enough to incorporate the proposed heterogeneities appropriately in a given reservoir system. It was then decided to select a much finer grid to generate the IPR data of horizontal and slanted wells producing from heterogeneous systems. After several trial runs using various grid sizes, a  $19 \times 3 \times 3$  grid was deemed to be appropriate and was selected to study the inflow performance of wells producing from heterogeneous reservoirs under solution-gas drive.

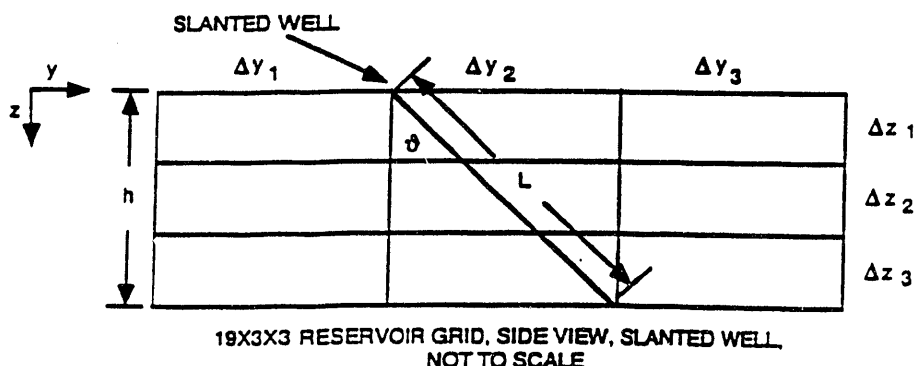
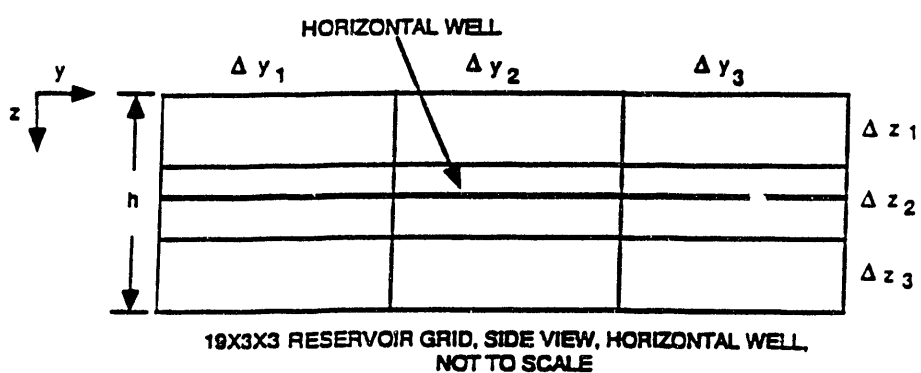
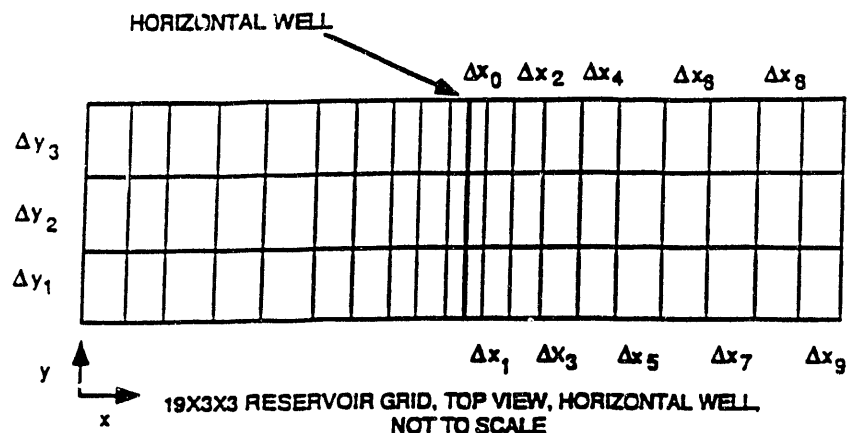
Figure 1 shows the  $19 \times 3 \times 3$  reservoir grid for generating the IPR data of horizontal and slanted wells. For a 20-acre well spacing as used in the base case data of Vogel<sup>1</sup>, the  $19 \times 3 \times 3$  grid had the following grid dimensions: constant geometric constant = 1.32,  $\Delta x_0$  (center block with wellbore) = 10 ft,  $\Delta y_{1-3} = 311.13$  ft, and  $\Delta z_{1-3} = 7.83$  ft. Table 2 shows the detailed grid block dimensions for the  $\Delta x$ ,  $\Delta y$ ,  $\Delta z$  variables of the  $19 \times 3 \times 3$  reservoir grid. The grid block sizes in the x-direction of the  $19 \times 3 \times 3$  grid were increased outward with a constant geometric factor from the center blocks containing the wellbore. The horizontal well was located in the center blocks and was oriented in the y direction of the grid (Fig. 1). The slanted well was positioned in the center column and was producing from the top, middle and bottom blocks in the base case (Fig. 1). This arrangement will retain more accuracy for flow computations in near-wellbore grid blocks where rapid pressure and saturation take place, and minimize the number of grid blocks and thus computer storage and execution time. However, the use of such a fine grid would significantly increase the computer CPU time for executing the simulation runs. For example, a single 500-day simulation run using the base case data of Vogel for a horizontal well with an automatic time step control option using a minimum and maximum time step of 0.01 and 3 days, could take more than 24 hours of turnaround time on the MicroVAX computer system. Because of the limited computing power for fine grid simulation, a very selected number of runs would be made to study the inflow performance of slanted/horizontal wells producing from heterogeneous systems. The runs would also focus on the inflow performance properties such as oil flow rate, gas-oil ratio, reservoir pressure, pressure and gas saturation profiles around the wellbore. Even with such a more focused study, the computing speed of the computer system was a big concern to the project. In March 1991, two new Digital high-speed workstations, the VAX station - 3100 Model 76, were installed in the MicroVAX II system. Each VAX station has a speed of 7.6 VPU and thus can provide more than 8 times the speed for executing the simulation runs. Practically, the turnaround time for the project simulations runs was reduced by a factor ranging from 10 to 20 times.

TABLE 2  
Reservoir Grid Block Dimensions Shown in  
Fig. 1

All  $\Delta x$ ,  $\Delta y$ , and  $\Delta z$  are in ft.

$\Delta x_0 = 10.00$
$\Delta x_1 = 13.20$
$\Delta x_2 = 17.40$
$\Delta x_3 = 23.00$
$\Delta x_4 = 30.40$
$\Delta x_5 = 40.10$
$\Delta x_6 = 53.00$
$\Delta x_7 = 70.00$
$\Delta x_8 = 92.40$
$\Delta x_9 = 122.20$
$\Delta y_1 = 311.13$
$\Delta y_2 = 311.13$
$\Delta y_3 = 311.13$
$\Delta z_1 = 7.83$
$\Delta z_2 = 7.83$
$\Delta z_3 = 7.83$

Using a  $19 \times 3 \times 3$  grid, and an automatic time step control with a minimum and maximum time step = 0.01 and 3 days (a time step of 0.001 day was used to initialize the simulation during the first 0.1 day), IPR results were obtained using the base case data of Vogel for a horizontal well under the six variables previously discussed. An examination of the inflow performance relationship (IPR) results indicates that the simulated IPR data to be somewhat unstable, i.e., fluctuating flow rate (or pressure) vs. time. The exact reasons for the unstable results were unclear. Probably the unstable results could have been due to the use of implicit pressure-explicit saturation (IMPES) formulation in the reservoir simulator to handle the rapid changes in pressure and saturation in the small grid blocks surrounding or enclosing the flowing horizontal well, which represent numerically difficult computations for IMPES. A possible remedy to reduce the unstable results is the use of an extremely small time step. An automatic time step control with a minimum and maximum time step = 0.01 and 3 days was selected for previous runs. It seems that the use of an automatic time step control for running the fine grid IPR simulations in this study caused unstable computations. The minimum and maximum time steps are not stringently and correctly selected during the course of simulation to ensure stable pressure and saturation solutions. For instance, at a certain time of



$\theta$  = SLANTED ANGLE    h = PAY THICKNESS =  $\Delta z_1 + \Delta z_2 + \Delta z_3$     L = TOTAL WELL LENGTH

Fig. 1 19 x 3 x 3 Reservoir grid and well orientation for horizontal and slanted wells.

simulation, an incorrect large time step is chosen for performing IMPES calculations and subsequently produces inaccurate results. Therefore, to generate more stable IPR results using the current simulator with an IMPES formulation, it is necessary to use a fixed small time step to execute the simulations. The use of a fixed time step was to avoid oscillating pressure and rate computations that occurred when a variable time step is used.

After several trial runs, a fixed time step of 0.01 day (14.4 minutes) appeared to be small enough to yield more stable results than the previously simulated values using an automatic time step selection. In this case, a fixed time step of 0.001 day was used to initialize the simulation during the first 0.1 day of simulation. With the use of such a small time step, generally a maximum of 50,000 time steps was required to generate an IPR data point for a horizontal well at a given flowing bottomhole pressure and cumulative oil production ranging from 0.1 to 10 % of the original oil in place. A maximum of 150,000 time steps was required to run a vertical well IPR study for a 19 x 19 x 1 grid. In this 19 x 19 x 1 grid,  $\Delta y_i = \Delta x_i$  of the 19 x 3 x 3 grid for the horizontal well where  $i$  is the row or column index, and  $\Delta z$  = total pay thickness = 23.5 ft. This translated into 16 CPU hours of VAX station time for one run. The execution of each of these small time step simulation runs was processed on the two newly installed high-speed work stations on the Micro-VAX II computer system; the results can be obtained in a reasonable turnaround time, e.g., less than 1 week for 15 horizontal well IPR simulation runs. Without these work stations, the turnaround time for each simulation run could take 10 to 20 times longer. In general, a horizontal well can deplete more than 10% OOIP from the 19 x 3 x 3 grid used in this study. However, for some unknown reasons, the simulator cannot deplete more than 6% OOIP for a well draining from the 19 x 19 x 1 grid.

The generated IPR results using the fixed small time step indicate that generally they appear to be more stable and reliable than the values obtained under the automatic time step control option. However, in some cases, the IPR results were still somewhat discontinuous, and it was beyond the scope of this study to investigate the exact reasons causing this. The NIPER horizontal simulator was developed by modifying the DOE - BOAST black oil reservoir simulator, which is known to have some stability problems when the gas phase saturations were high in the reservoir. Again, the unstable results could have been simply due to the use of IMPES formulation to handle the numerically difficult problems of oil and gas flow in small grid blocks as discussed before.

Based on the IPR plots of a horizontal well and two slanted wells for the base case with equal vertical and horizontal permeability ( $k_v = k_h$ ) generated in this study (presented in later sections), it seems that a high  $k_v$  causes a significant cross flow around the horizontal or slanted wellbore. Because of this high cross flow and the usually much longer horizontal wellbore drainage length exposed to formation than the vertical well, the inflow performance in a longer horizontal or slanted well can be unstable in certain circumstances. The IPR plots for the  $k_v = 0.1 k_h$

case for the horizontal and the two slanted wells shown in figures 11, 20, and 29, display more stability than the ones with  $k_v = k_h$  case shown in figures 10, 19, and 28. This indicates that less gas cross flow will lead to more stability in the inflow performance results.

### General Physical Interpretation of IPR Curves

Based on the generated IPR data in this study and the Vogel IPR curve, the generated IPR results or curves follow the typical behavior of a solution gas drive reservoir. The basic physical interpretations of an IPR curve are as follows. A normalized IPR curve is a plot of normalized flowing bottomhole pressure  $p'$  (y-axis) vs. normalized oil flow rate  $q'$  (x-axis), with  $p' = p_{wf}/p_r$  and  $q' = q_o/q_{omax}$ , where  $p_{wf}$  = flowing bottomhole pressure,  $p_r$  = average reservoir pressure,  $q_o$  = oil flow rate, and  $q_{omax}$  = maximum oil flow rate. The inverse slope of an IPR curve,  $dq/dp$  or  $q/dp$ , represents the oil productivity index or can be viewed as a quantity proportional to the index. Theoretically, for a one-phase (oil) flow case, fluid flow follows Darcy equation the oil productivity index is constant, and the IPR curve will be a straight line. For a two-phase flow (oil and gas) where the critical gas saturation is reached, as pressure depletes, more gas evolves from the liquid oil and oil saturation decreases and gas saturation increases, assuming the water saturation remains constant.

The saturation change leads to an increase in relative permeability ratio  $k_{rg}/k_{ro}$ , where  $k_{rg}$  is the gas relative permeability and  $k_{ro}$  is the oil relative permeability. Also the viscosity ratio  $m_o/m_g$  is extremely high, where  $m_o$  and  $m_g$  are oil and gas viscosity respectively. For instance, at low pressures, this ratio can be as high as 100 and even at high pressures the ratio will be high.<sup>9</sup> Therefore, as pressure declines in two-phase flow, the rapid increase in the permeability and viscosity ratios impedes the oil flow drastically. This translates into a decrease in oil productivity index with decrease in flowing bottomhole pressure. Mathematically, this means that an IPR curve slope increases with decrease in pressure. This explains why the original Vogel IPR curve for a vertical well is concave to the right when  $p'$  decreases. A useful variable that may be used to predict concavity or curvature or shifting of an IPR curve to right or left is the producing gas-oil ratio (GOR). In general, for an oil reservoir starting production at an initial pressure the same as the saturation pressure, as the oil depletion ( $N_p/N$ ) increases, the subsurface reservoir gas saturations increases and the GOR increases, and the IPR curvature increases or shifts to right. In Vogel's<sup>1</sup> original work, the IPR curves for  $N_p/N = 0.1, 2, 4, 6, 8$  and 10% overlay each other, and it is unclear whether the IPR curve shifts from left to right or right to left. Up to a certain depletion stage, e.g.,  $N_p/N = 8\%$ , the gas phase becomes the dominant one, and decline of reservoir pressure is not as rapid as in the beginning; the result is a less rapid decline in oil productivity index as flowing bottomhole pressure decreases. The IPR curve loses its curvature as reported by

Vogel for  $N_p/N > 10\%$ . The IPR curve shifts to left under this condition. The shift of IPR curve from left to right for  $0\% < N_p/N < 8\%$  and then right to left as  $N_p/N > 8\%$  is also found in the base case horizontal IPR curves generated from this study and Bendakhlia and Aziz.<sup>7</sup> This close agreement of the shift of IPR curves in both studies verifies the validity of the NIPER horizontal well reservoir simulator. It is the subsurface two-phase flow condition that governs the ultimate IPR curve shape. The most critical parameter is the gas saturation  $S_g$  distributions surrounding the wellbore.

Figures 2, 3, and 4, show for the base case horizontal well, the change of reservoir pressure, oil flow rate, and gas-oil ratio (GOR), with cumulative oil production under two flowing bottomhole pressures  $p_{wf}$  of 100 psia (85.3 psig) and 600 psia (585.3 psig), respectively. Based on these figures, the following was observed. As  $N_p/N$  increases from 0 to 6%, reservoir pressure decreases rapidly. For  $N_p/N > 6\%$ , the rate of decline of reservoir pressure begins to drop (Fig. 2). The gas phase becomes dominant and the pressure decline is not as significant as at the beginning depletion stage. Also shown in Fig. 2, the reservoir pressure is independent of the flowing bottomhole pressure and is affected by the amount of the oil depleted. This would have been expected from the concept of oil material balance. Oil production rate of the horizontal well drops drastically to less than 20% of its initial rate after only 2 % of the oil-in-place is depleted (Fig. 3). However, the oil rate will then decline at a lower rate. Figure 3 also shows that after 4% oil depletion, the oil production rates for  $p_{wf} = 100$  and 600 psia are almost identical. This implies that a lower wellbore pressure drawdown can attain the same oil flow rates as those obtained from higher pressure drawdown. Therefore for  $N_p/N > 6\%$ , the reservoir pressure and oil flow rate decline begin to drop, and accordingly the oil oil productivity index decreases at a lower rate than that at the beginning depletion stage. So the IPR curve will appear to be less concave and shift from right to left for higher  $N_p/N$ . This is in agreement of the shifting of IPR curves presented above. Figure 4 indicates that the GOR for both  $p_{wf}$  increase with oil depletion. As discussed above, the IPR curve for a horizontal well shifts from right to left for  $N_p/N > 8\%$ . Therefore, an increase in GOR will not necessarily imply the IPR curve shift from left to right but will also depend on the time of or oil depletion stage.

### Comparison of Pressure and Gas Saturation Profiles for Vertical and Horizontal Wells

The reservoir pressure and gas saturation distributions (or profiles) of the base case vertical and horizontal wells were generated at cumulative oil production  $N_p/N = 0.1$  and 6%. These distributions and the related inflow performance relationship (IPR) simulation results were used to aid in explaining the fundamental inflow phenomenon of these wells.

Figures 5 and 6 compare the reservoir grid pressure and gas saturations along the distance (x-direction of reservoir

grid) from the wellbore respectively for the vertical and horizontal wells at a flowing bottomhole pressure  $p_{wf}$  of 100 psia. Figures 7 and 8 show these comparisons at  $p_{wf} = 600$  psia. At 0.1% oil depletion, which almost represents the very beginning of the oil production, Fig. 7 shows that the horizontal well in general has a higher pressure along the x-direction wellbore distance while the vertical well has a lower pressure around the wellbore. This corresponds to a lower and higher gas saturation for the horizontal and vertical well respectively (Fig. 8). Fig. 9 shows the IPR curves for vertical and horizontal wells at  $N_p/N = 0.1\%$ , indicating the horizontal IPR curve at 0.1% depletion is more linear than the vertical well IPR curve and is on its left. This can be explained by Figs. 5 and 6. The relatively lower gas saturation distributions around the horizontal wellbore than the vertical wellbore leads to a less concave IPR curve and is shown in Fig. 9. The pressure and gas saturation profiles for  $p_{wf} = 600$  psia are quite similar to the one at  $p_{wf} = 100$  psia. In the  $p_{wf} = 600$  psia case, the differences between the corresponding vertical and horizontal well saturation profiles are not as big as the  $p_{wf} = 100$  psia case. This will be expected as a higher pressure drawdown at  $p_{wf} = 100$  psia will lead to a higher gas saturation distributions around the wellbore than the relatively lower drawdown at  $p_{wf} = 600$  psia case. Based on the current findings, the gas saturations around the wellbore is the critical parameter to determine the shape or slope and oil productivity index of an IPR curve for both vertical and horizontal wells.

### IPR Results of Horizontal and Slanted Wells

The following presents the normalized IPR curves ( $p'$  vs.  $q'$ ) at  $N_p/N = 0.1, 2, 4, 6, 8, 10\%$  for the horizontal and slanted well base cases and under the following six variables, vertical permeability, eccentricity, and stratification, perforated length, and formation thickness, and heterogeneous permeability. A  $19 \times 3 \times 3$  grid and a fixed time step of 0.01 day (a time step of 0.001 day) was used to initialize the simulation for the first 0.1 day) were used to generate the IPR data. Recall that normalized pressure  $p' = p_{wf}/p_r$  and normalized rate  $q' = q_0/q_{0max}$ , where  $p_{wf}$  = flowing bottomhole pressure,  $p_r$  = average reservoir pressure,  $q_0$  = oil flow rate, and  $q_{0max}$  = maximum oil flow rate, and  $N_p/N$  = cumulative oil production.

### Horizontal Well IPR

#### Base Case

Figure 10 shows the IPR curves using the base case data of Vgel. The horizontal well is located in the middle of the  $19 \times 3 \times 3$  grid and draining from the middle of the pay zone. In general, the IPR curves appear to be continuous and stable. As  $N_p/N$  increases, the IPR curve of a producing horizontal well shifts to the right and has more concavity or curvature. However, as  $N_p/N$  increases from

8 to 10%, the IPR curve begins to lose its concavity as shown by the IPR curve at  $N_p/N = 10\%$ . This curve almost overlaps the 2% IPR curve for  $p' > 0.4$  and the 0.1% IPR curve for  $p' < 0.4$ . The shift of the IPR curve from left to right and then right to left have been explained in detail previously. Likewise, the base case horizontal well IPR curves are quite similar to those presented by Bendakhila and Aziz.<sup>7</sup>

### Vertical Permeability

Figure 11 shows the IPR curves for the vertical permeability case. A vertical permeability  $k_v$  and horizontal permeability  $k_h$  of 2 and 20 mD, respectively, were used and  $k_v = 0.1 k_h$ . In general, the IPR curves as shown in Fig. 11 are stable with the exception of the 10% curve where there is a discontinuity at  $p' = 0.4$ . As discussed, lower gas cross flow leads to more stable IPR results generated by the horizontal well simulator. Generally, the IPR curve shifts to the right as  $N_p/N$  increases from 0 to 8 % until which the IPR curve goes to the left as shown by the 10% IPR curve. These IPR curves appear to follow the pattern of those of the base case.

### Eccentricity

Two cases were studied: the horizontal wellbore is located in the bottom or top layer of the  $19 \times 3 \times 3$  grid. Figure 12 shows the the IPR curves for the bottom layer case. In general, the IPR curves as shown in Fig. 12 are stable. Generally, the IPR curve shifts to the right as  $N_p/N$  increases from 0.1 to 8% until which the IPR curve goes to the left as shown by the 10% IPR curve. These IPR curves appear to follow the pattern of those of the base case. However, these IPR curves generally have more concavity than the base case curves. Figure 13 shows the IPR curves for the top layer case. These IPR curves follow the pattern of those of the bottom layer case. However, the IPR data for  $p' < 0.5$  for  $N_p/N = 2, 4$ , and 10% cases are different from the bottom layer case data.

### Stratification

Two cases were studied: two stratified reservoir systems each with three different strata permeabilities are used: 40, 20 and 10 md for the top, middle and bottom layers, respectively, for the first system, and 10, 20 and 40 md for the top, middle and bottom layers, respectively, for the second system. Figure 14 shows the IPR curves for the first stratified system. In general, the IPR curves as shown in figure 14 are stable. Generally, the IPR curve shifts to the right as  $N_p/N$  increases from 0.1 to 8% until which the IPR curve goes to the left as shown by the 10% IPR curve. Interestingly, the IPR curves at  $N_p/N = 0.1, 2$ , and 10% overlap each other in almost all ranges of  $p'$ . In general, the IPR curves of the stratified system 1 appear to follow the pattern of those of the base case. Figure 15 shows the IPR curves for the second stratified system.

These curves are quite different than those of the first stratified system. They display more concavity and appear to be less stable as shown in Fig. 15. In general, for a horizontal reservoir system, gas evolved from the oil in the lower part of the pay zone will flow to the top of the reservoir system. As the bottom layer has the highest permeability among the three layers in the grid for the second system, it will allow gas to flow more easily to the wellbore than the first stratified system case where the bottom layer has the lowest permeability. Thus a higher gas saturation is expected in the second system and the IPR curves appear more concave than the first one.

### Perforated Length

The perforated horizontal length  $L_p$  is 311 ft while the total horizontal length of the well  $L_h$  is 933 ft, and  $L_p = 1/3 L_h$ . The perforated length is located in the center of the  $19 \times 3 \times 3$  grid (Fig. 1). Figure 16 shows the IPR curves for this selected perforated length case. The IPR curve for  $N_p/N = 0.1\%$  case appears to be more linear than all the other IPR curves which almost overlap each other at any  $p'$  with the exception of the 8 % curve. The IPR curve for  $N_p/N = 0.1\%$  case is very similar to the one in the base case. The other IPR curves are similar to the one at  $N_p/N = 8\%$  in the base case.

### Formation Thickness

A formation thickness of 235 ft is used, which is 10 times that of the base case (23.5 ft). Thus, the horizontal well is producing from a thick-pay reservoir where gravity drainage may have a more dominant effect on oil production than a thin-pay system. Figure 17 shows the IPR curves for this formation thickness case. IPR curves of this thick-pay reservoir are smooth, and all of them appear to be fairly linear. In particular, the IPR curve for  $N_p/N = 0.1\%$  case is highly linear. Generally, the IPR curve shifts to the right as  $N_p/N$  increases from 0 to 8 % until which the IPR curve goes to the left as shown by the 10% IPR curve. These IPR curves appear to follow the pattern of those of the base case.

### Heterogeneous Permeability

Under this heterogeneous permeability case, a reservoir system with a gradual change in x-direction permeability was selected. This is represented by various reservoir grid column permeability values. The data used are 103.20, 86.00, 71.66, 59.72, 49.77, 41.47, 34.56, 28.80, 24.00, 20.00, 16.00, 12.80, 10.24, 8.19, 6.55, 5.24, 4.19, 3.36, and 2.68 md, representing a 20% decrease in permeability from left to right of the  $19 \times 3 \times 3$  reservoir grid. Figure 18 shows the IPR curves for this heterogeneous permeability case. Generally the IPR curves shift from left to right. Except the 2% curve at  $p' = 0.5$ , the IPR curves appear to be fairly stable. They are less concave than the base case.

## Slanted Well IPR

Two slanted angles were used in the generation of IPR data for the slanted well case: 85.68 and 75 degrees. From the previous SGP27 project study, it was found that IPR curves are similar for a slanted well with an angle of less than 45 degrees. As the use of a fine grid to generate IPR data can be extremely time consuming, it was decided to generate the IPR data using only two angles greater than 45 degrees. The wellbore geometry of a slanted well in this study is illustrated in Fig. 1.

### 85.68 Degree - Slanted well

The following discussion presents the normalized IPR curves ( $p'$  vs.  $q'$ ) at  $N_p/N = 0.1, 2, 4, 6, 8, 10\%$  for the 85.68 degree-slanted well base case and under the following six variables, vertical permeability, eccentricity, and stratification, perforated length, and formation thickness. A  $19 \times 3 \times 3$  grid and a fixed time step of 0.01 day (a time step of 0.001 day was used to initialize the simulation for the first 0.1 day) were used to generate the IPR data. An examination of the normalized IPR plots of the slanted well indicates that the simulated IPR data generally to be more concave than those of the horizontal well case. This increase in concavity could indicate a more gaseous flow in the slanted well than the horizontal well. This is justified because one-third of the slanted well in this  $19 \times 3 \times 3$  grid was producing from the top layer of the reservoir system where gas saturation would be higher than the middle layer. In the previous base case for the horizontal well, the well was producing from the middle layer. Also generally the simulated IPR results for the slanted well case appear to be more unstable than those of the horizontal case.

### Base Case

Figure 19 shows the IPR curves using the base case data of Vogel. The slanted well is located in the middle row of the  $19 \times 3 \times 3$  grid and draining from the center portion of the reservoir pay zone (Fig. 1). The 0.1% IPR curve is similar to the horizontal well base case one, and is fairly linear. Other than the 0.1% case, in general, the IPR curves display more concavity and appear to be more unstable than the ones in the horizontal well case. Figure 19 shows that the maximum concavity occurs at the  $N_p/N = 2\%$  and then the IPR curves shift to the left as  $N_p/N$  increases.

### Vertical Permeability

Figure 20 shows the IPR curves for the vertical permeability case. A vertical permeability  $k_v$  and horizontal permeability  $k_h$  of 2 and 20 md, respectively, were used and  $k_v = 0.1 k_h$ . In general, the IPR curves as shown in figure 20 are much more stable than the base case. Generally, the IPR curve shifts to the right as  $N_p/N$  increases from 0 to 6% until which the IPR curve goes to

the left as shown by the 8 % IPR curve and then goes to the right at  $N_p/N = 10\%$ . With the exception of the 0 and 8% IPR curves, all the other IPR curves almost overlap each other.

### Eccentricity

Two cases were studied: the slanted wellbore is located in the bottom or top layer of the  $19 \times 3 \times 3$  grid. Figure 21 shows the the IPR curves for the bottom layer case. In general, the IPR curves as shown in figure 21 are stable. Generally, the IPR curve shifts to the right as  $N_p/N$  increases from 0.1 to 8% until which the IPR curve goes to the left as shown by the 10% IPR curve. These IPR curves appear to follow the pattern of those of the base case. However, these IPR curves generally have more concavity than the base case curves. Figure 22 shows the IPR curves for the top layer case. These IPR curves follow the pattern of those of the bottom layer case. However, the IPR data for  $p' < 0.5$  for  $N_p/N = 2, 4$ , and 10% cases are different from the bottom layer case data.

### Stratification

Two cases were studied: two stratified reservoir system each with three different strata permeabilities are used: 40, 20 and 10 md for the top, middle and bottom layers, respectively, for the first system, and 10, 20 and 40 md for the top, middle and bottom layers, respectively, for the second system. Figure 23 shows the IPR curves for the first stratified system. In general, the IPR curves as shown in figure 23 are stable. Generally, the IPR curve shifts to the right as  $N_p/N$  increases from 0.1 to 4% until which the IPR curve goes to the left as shown by the 10 % IPR curve. Figure 24 shows the IPR curves for the second stratified system. These curves are quite different than those of the first stratified system. Except for the 0.1% case.

### Perforated Length

The perforated length  $L_p$  is 104 ft while the total length of the slanted well  $L_s$  is 312 ft, and  $L_p = 1/3 L_s$ . The perforated length is located in the center of the  $19 \times 3 \times 3$  grid. Figure 25 shows the IPR curves for this selected perforated length case. The IPR curve for  $N_p/N = 0.1\%$  case appears to be more linear than all the other IPR curves which almost overlap each other at any  $p'$  with the exception of the 8% curve. The IPR curve for  $N_p/N = 0.1\%$  case is very similar to the one in the base case. Generally the IPR curves are less than concave than those in the base case. This is expected as the one-third wellbore is located in the center of the reservoir grid and is not draining from the top zone which has a higher gas saturation.

### Formation Thickness

A formation thickness of 235 ft is used, which is 10 times that of the base case (23.5 ft). Thus, the slanted well is producing from a thick-pay reservoir where gravity drainage may have a more dominant effect on oil production than a thin-pay system. Figure 26 shows the IPR curves for this formation thickness case. IPR curves of this thick-pay reservoir are smooth, and all of them appear to be fairly linear. In particular, the IPR curves for  $N_p/N = 0.1$  and 8% case are highly linear. The 6% IPR curve has the maximum concavity.

### Heterogeneous Permeability

Under this heterogeneous permeability case, a reservoir system with a gradual change in x-direction permeability was selected. This is represented by various reservoir grid column permeability values. The data used are 103.20, 86.00, 71.66, 59.72, 49.77, 41.47, 34.56, 28.80, 24.00, 20.00, 16.00, 12.80, 10.24, 8.19, 6.55, 5.24, 4.19, 3.36, and 2.68 md, representing a 20 % decrease in permeability from left to right of the  $19 \times 3 \times 3$  reservoir grid. Figure 27 shows the IPR curves for this heterogeneous permeability case. The 0.1% IPR curve is fairly linear. All the other IPR curves except the 10 % one almost overlay each other. The 10% curve displays serious discontinuity for  $p' < 0.6$ . Generally the IPR curves are more concave than the corresponding ones in the horizontal well case.

### 75 Degree - Slanted Well

The following presents the normalized IPR curves ( $p'$  vs.  $q'$ ) at  $N_p/N = 0.1, 2, 4, 6, 8, 10\%$  for the 75 degree-slanted well base case and under the following six variables, vertical permeability, eccentricity, and stratification, perforated length, and formation thickness. A  $19 \times 3 \times 3$  grid and a fixed time step of 0.01 day (a time step of 0.001 day was used to initialize the simulation for the first 0.1 day) were used to generate the IPR data.

An examination of the normalized IPR plots of the 75-degree slanted well indicates that the simulated IPR data generally to be slightly more concave than those of the horizontal well case. As in the case of the 85.68-degree slanted well, this increase in concavity could indicate a more gaseous flow in the slanted well than the horizontal well. This is justified because one-third of the slanted well in this  $19 \times 3 \times 3$  grid was producing from the top layer of the reservoir system where gas saturation would be higher than the middle layer. In the previous base case for the horizontal well, the well was producing from the middle layer. In general, the IPR curves for the 75-degree slanted well are similar to those of the 85.68-degree slanted well. However, compared to the 85.68-degree case, less concavity is displayed in the 75-degree well case. The wellbore length for production for the 75-degree well is 91

ft in the base case and is more than 3 times shorter than the one in the 85.68-degree well, 312 ft.

### Base Case

Figure 28 shows the IPR curves using the base case data of Vogel. The slanted well is located in the middle row of the  $19 \times 3 \times 3$  grid and draining from the center portion of the reservoir pay zone (Fig. 1). The 0.1% IPR curve is similar to the horizontal well base case one, and is fairly linear. Other than the 0.1% case, in general, the IPR curves display more concavity and appear to be more unstable than the ones in the horizontal well case. Figure 28 shows that the maximum concavity occurs at the  $N_p/N = 2\%$  and then the IPR curves shift to the left as  $N_p/N$  increases.

### Vertical Permeability

Figure 29 shows the IPR curves for the vertical permeability case. A vertical permeability  $k_v$  and horizontal permeability  $k_h$  of 2 and 20 md, respectively, were used and  $k_v = 0.1 k_h$ . In general, the IPR curves as shown in figure 29 are much more stable than the base case. Generally, the IPR curve shifts to the right as  $N_p/N$  increases from 0 to 6 % until which the IPR curve goes to the left as shown by the 8% IPR curve and then goes to the right at  $N_p/N = 10\%$ . With the exception of the 0 and 8% IPR curves, all the other IPR curves almost overlap each other.

### Eccentricity

Two cases were studied: the slanted wellbore is located in the bottom or top layer of the  $19 \times 3 \times 3$  grid. Figure 30 shows the the IPR curves for the bottom layer case. In general, the IPR curves as shown in figure 30 are stable. Generally, the IPR curve shifts to the right as  $N_p/N$  increases from 0.1 to 8% until which the IPR curve goes to the left as shown by the 10% IPR curve. These IPR curves appear to follow the pattern of those of the base case. However, these IPR curves generally have more concavity than the base case curves. Figure 31 shows the IPR curves for the top layer case. These IPR curves follow the pattern of those of the bottom layer case. However, the IPR data for  $p' < 0.5$  for  $N_p/N = 2, 4$ , and 10% cases are different form the bottom layer case data.

### Stratification

Two cases were studied: two stratified reservoir system each with three different strata permeabilities are used: 40, 20 and 10 md for the top, middle and bottom layers, respectively, for the first system, and 10, 20 and 40 md for the top, middle and bottom layers, respectively, for the second system. Figure 32 shows the IPR curves for the first stratified system. In general, the IPR curves as shown in Fig. 32 are stable. Generally, the IPR curve shifts to

the right as  $N_p/N$  increases from 0.1 to 4% until which the IPR curve goes to the left as shown by the 10% IPR curve. Figure 33 shows the IPR curves for the second stratified system. These curves are quite different than those of the first stratified system. Except the 0.1% IPR curve, all other curves almost overlay each other.

### Perforated Length

The perforated length  $L_p$  is 30.3 ft while the total length of the slanted well  $L_s$  is 91 ft, and  $L_p = 1/3 L_s$ . The perforated length is located in the center of the  $19 \times 3 \times 3$  grid. Figure 34 shows the IPR curves for this selected perforated length case. The IPR curve for  $N_p/N = 0.1\%$  case appears to be more linear than all the other IPR curves which almost overlap each other at any  $p'$  with the exception of the 8% curve. The IPR curve for  $N_p/N = 0.1\%$  case is very similar to the one in the base case. Generally the IPR curves are less than concave than those in the base case. This is expected as the one-third wellbore is located in the center of the reservoir grid and is not draining from the top zone which has a higher gas saturation.

### Formation Thickness

A formation thickness of 235 ft is used, which is 10 times that of the base case (23.5 ft). Thus, the slanted well is producing from a thick-pay reservoir where gravity drainage may have a more dominant effect on oil production than a thin-pay system. Figure 35 shows the IPR curves for this formation thickness case. IPR curves of this thick-pay reservoir are smooth, and all of them appear to be fairly linear. In particular, the IPR curves for  $N_p/N = 0.1$  and 8% case are highly linear. The 6% IPR curve has the maximum concavity.

### Heterogeneous Permeability

For this heterogeneous permeability case, a reservoir system with a gradual change in x-direction permeability was selected. This is represented by various reservoir grid column permeability values. The data used are 103.20, 86.00, 71.66, 59.72, 49.77, 41.47, 34.56, 28.80, 24.00, 20.00, 16.00, 12.80, 10.24, 8.19, 6.55, 5.24, 4.19, 3.36, and 2.68 md, representing a 20 % decrease in permeability from left to right of the  $19 \times 3 \times 3$  reservoir grid. Figure 36 shows the IPR curves for this heterogeneous permeability case. The 0.1% IPR curve is fairly linear. All the other IPR curves except the 10% one almost overlay each other. Similar to the 85.68 degree-slanted well case, the 10% curve displays serious discontinuity for  $p' < 0.5$ . Generally the IPR curves are less concave than the corresponding ones in the 85.68-degree well case.

### IPR Data Interpolation and Software

The normalized IPR data generated in this study were installed in a PC software called IPR program. The

program uses cubic spline technique to interpolate the dimensionless  $q_i'$  at a given dimensionless  $p_i'$ . Also, the program can show the IPR curves generated in this study on the computer screen and print hard copies. Therefore, a user can overlay his actual normalized IPR data on the computer generated curve and make comparisons. The software and the user's manual are submitted to the Department of Energy as a separate deliverable.<sup>10</sup> Details of the program usage and applications can be found in the user's manual.

### Results and Conclusions

1. Inflow performance relationships (IPRs) for horizontal and slanted wells producing under solution-gas drive mechanism were generated using NIPER's vertical/horizontal/slanted well reservoir simulator under six different variables: vertical permeability, wellbore eccentricity, stratification, perforated length, formation thickness, and heterogeneous permeability.
2. All IPR curves at cumulative oil production  $N_p/N = 0.1\%$  or during the very early production stage of the horizontal and slanted wells display a linear behavior. Most IPR curves beyond  $N_p/N = 2\%$  display concavity that is similar to the Vogel IPR curve for a vertical well.
3. Inflow performance relationship (IPR) curves of vertical, horizontal, and slanted wells producing from solution-gas drive follow the general behavior of solution-gas drive mechanism. The initial shifting of IPR curves from left to right is due to the increase of gas saturation around the wellbore. After the well has depleted a certain amount, e. g., 8%, the shift of the IPR curve is from right to left. At this time, the gas phase dominates the two-phase (oil and gas) flow and reservoir pressure and oil productivity index decline are small, which result in a less concave IPR curve.
4. The IMPES formulated horizontal well reservoir simulator can produce unstable IPR results for a fine reservoir grid in some cases even when a small fixed time step of 0.01 day was used.

### References

1. Vogel, J. V. Inflow Performance Relationships for Solution Gas Drive Wells. *J. Pet. Tech.*, January 1968, pp. 83 - 93.
2. Cheng, A. M. *Development of an Inflow Performance Relationship (IPR) for a Slanted/Horizontal Well* DOE Report NIPER - 458, January 1990.
3. Cheng, A. M. *Inflow Performance Relationships for Solution-Gas-Drive Slanted/Horizontal Wells*. Pres. at the SPE Annual Tech. Conf. and Exhibition, New Orleans, Sept. 23 - 26, 1990. SPE Paper 20720.
4. Chang, M. M. *Simulation of Production from Wells with Horizontal/Slanted Laterals*. DOE Report NIPER-326 (Revised), October, 1988.

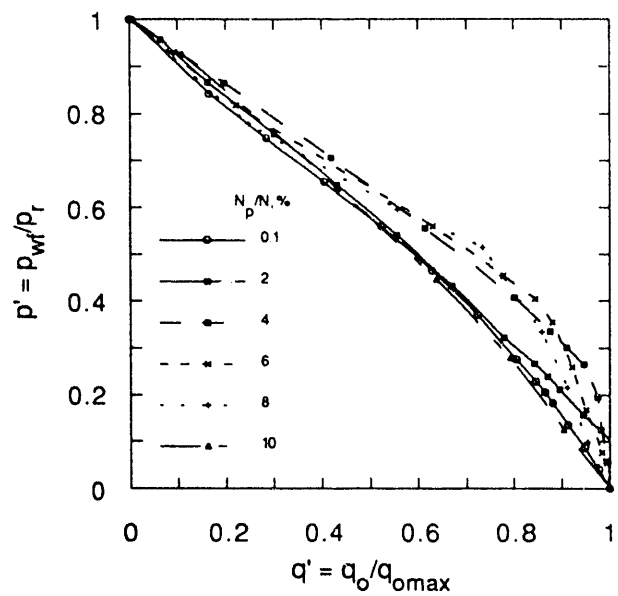


Fig. 14 Horizontal well inflow performance relationship; strata permeability = 40, 20, 10 mD (top, middle, and bottom).

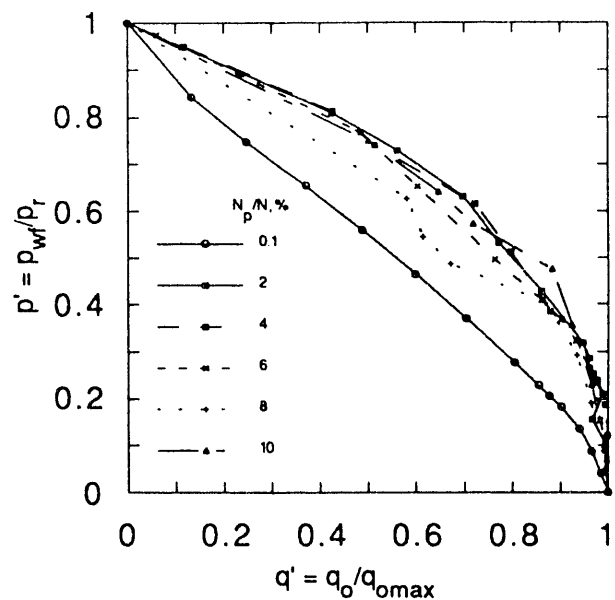


Fig. 16 Horizontal well inflow performance relationship; perforated length =  $1/3 \times$  total well length.

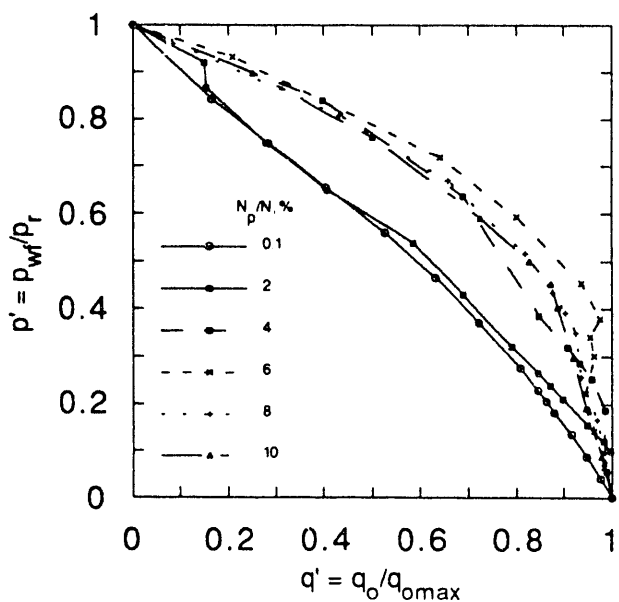


Fig. 15 Horizontal well inflow performance relationship; strata permeability = 10, 20, 40 mD (top, middle, and bottom).

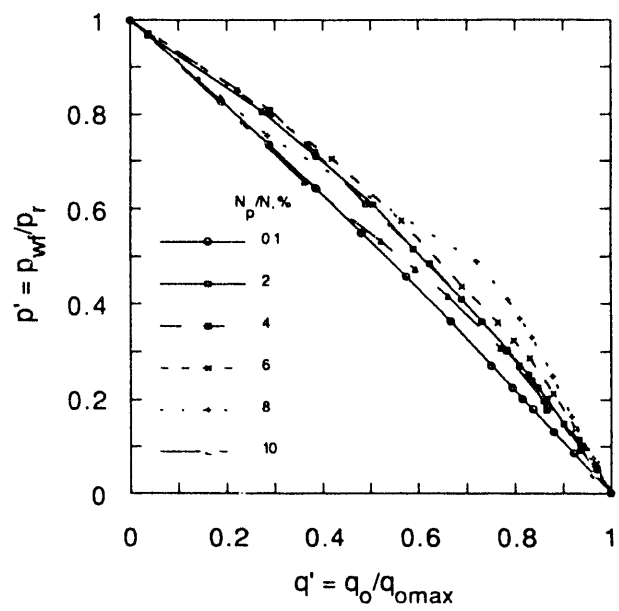


Fig. 17 Horizontal well inflow performance relationship; formation thickness = 235 ft = 10  $\times$  base case.

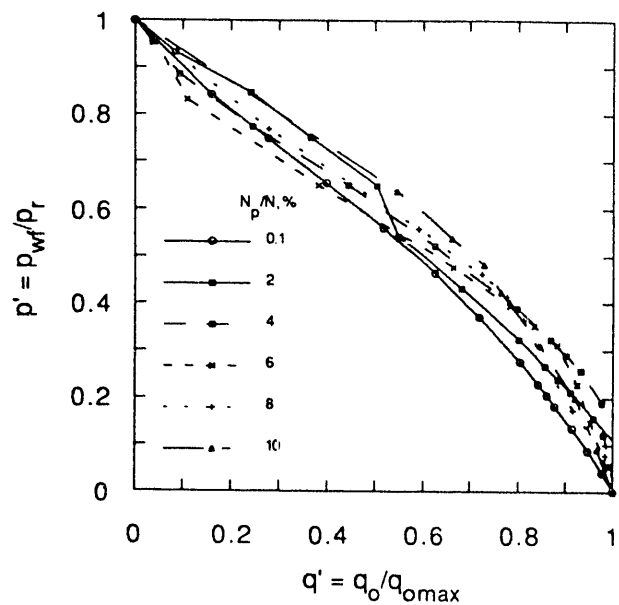


Fig. 18 Horizontal well inflow performance relationship; heterogeneous permeability, permeability decreases from left to right by 20%.

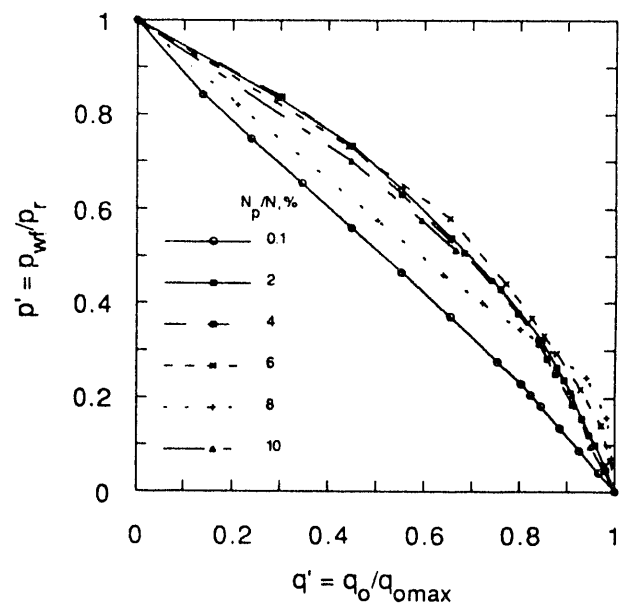


Fig. 20 85.68-Deg Slanted well inflow performance relationship; vertical permeability =  $0.1 \times$  horizontal permeability.

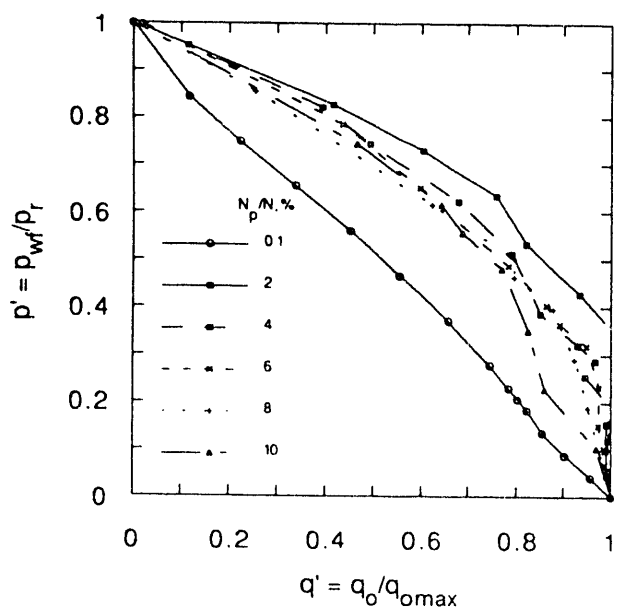


Fig. 19 85.68-Deg Slanted well inflow performance relationship; base case.

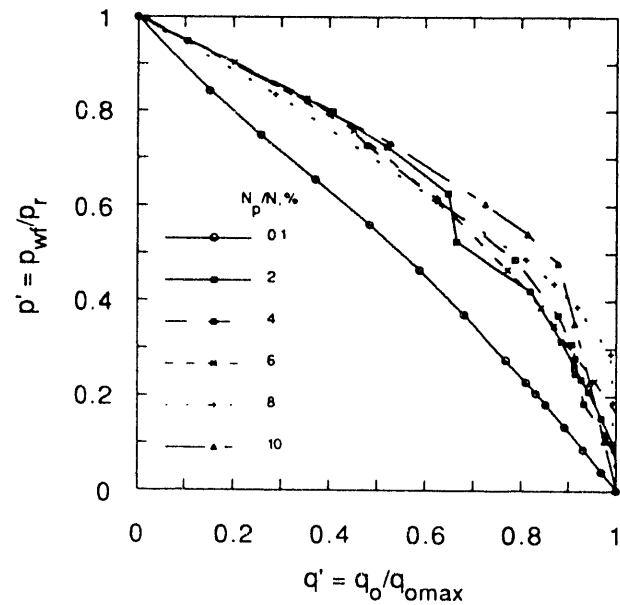


Figure 21. 85.68-Deg Slanted well inflow performance relationship; wellbore in bottom layer of  $19 \times 3 \times 3$  grid.

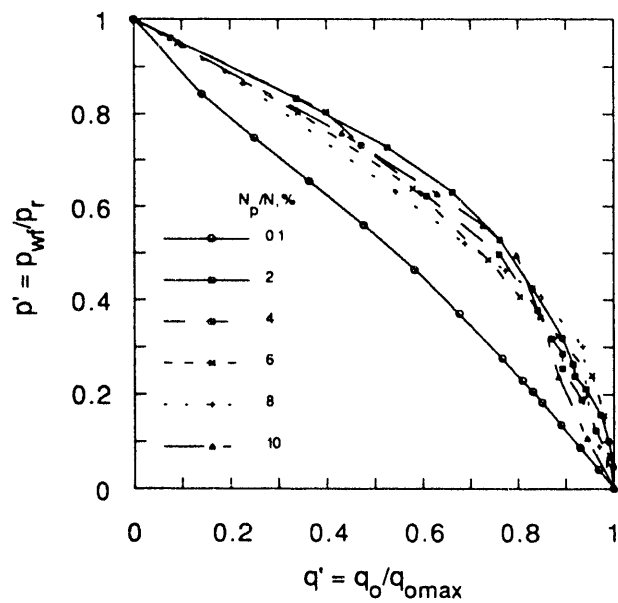


Fig. 22 85.68-Deg Slanted well inflow performance relationship; wellbore in top layer of  $19 \times 3 \times 3$  grid.

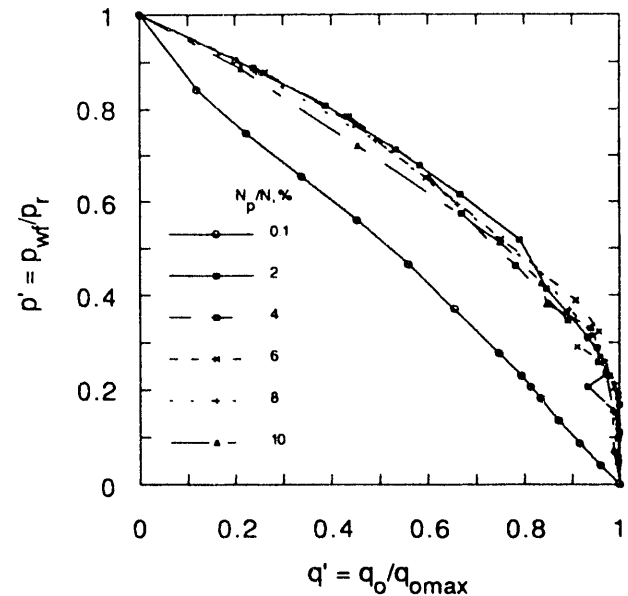


Fig. 24 85.68-Deg Slanted well inflow performance relationship; strata permeability = 10, 20, 40 mD (top, middle, and bottom).

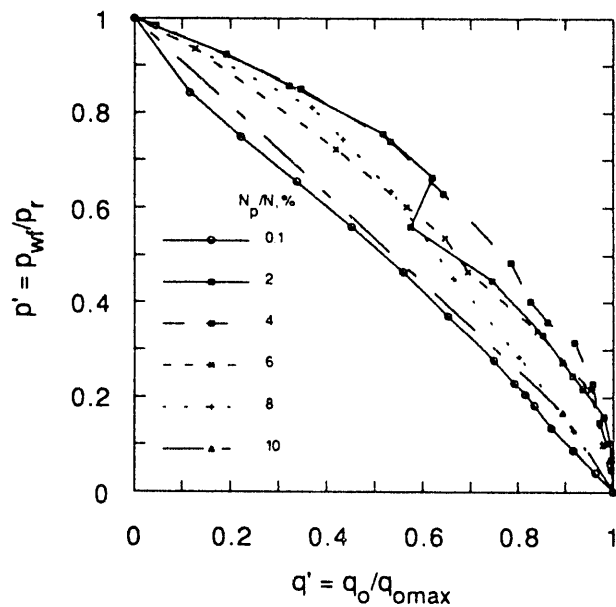


Fig. 23 85.68-Deg Slanted well inflow performance relationship; strata permeability = 40, 20, 10 mD (top, middle, and bottom).

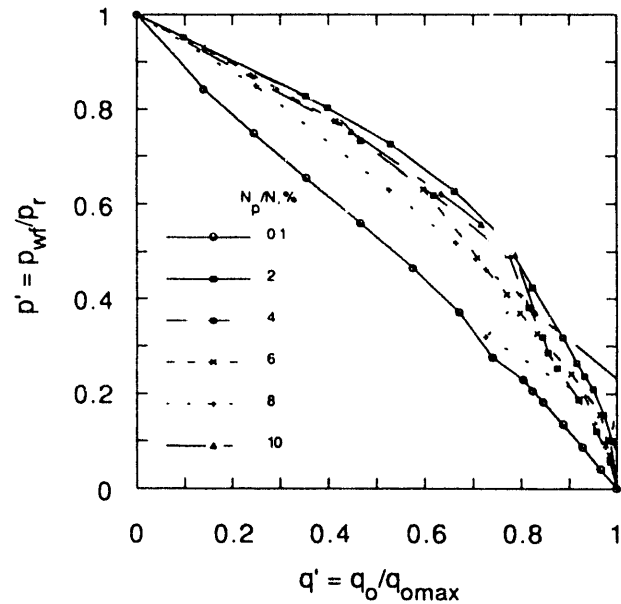


Fig. 25 85.68-Deg Slanted well inflow performance relationship; perforated length =  $1/3 \times$  total well length.

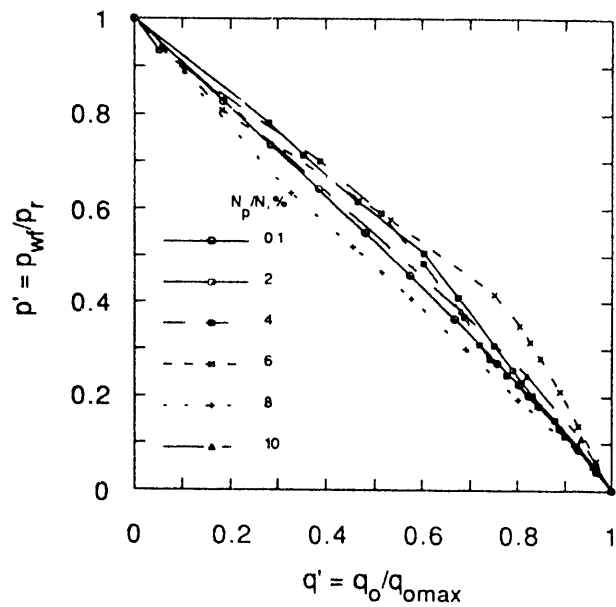


Fig. 26 85.68-Deg Slanted well inflow performance relationship; formation thickness = 235 ft = 10 x base case.

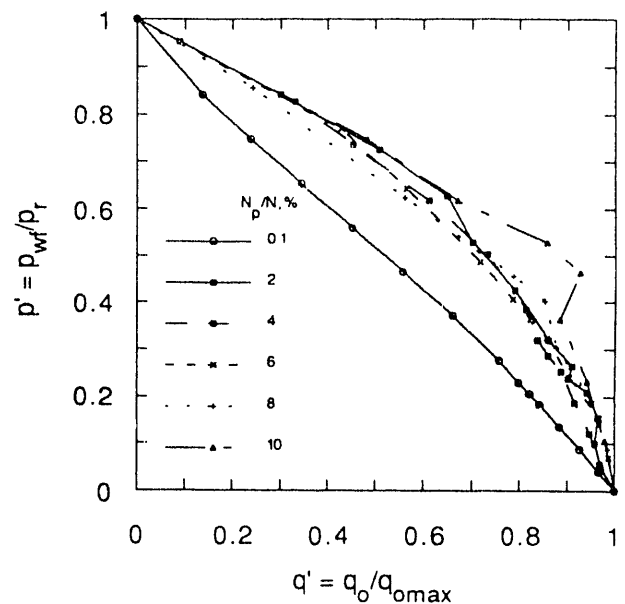


Fig. 28 75-Deg Slanted well inflow performance relationship; base case.

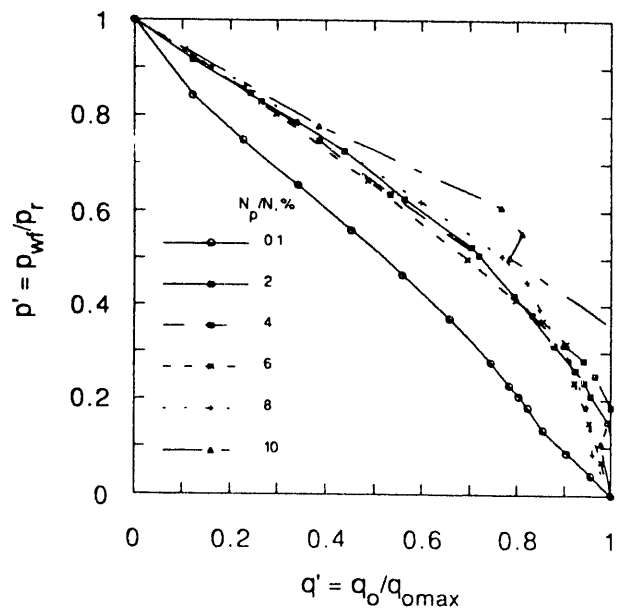


Fig. 27 85.68-Deg Slanted well inflow performance relationship; heterogeneous permeability, permeability decreases from left to right by 20%.

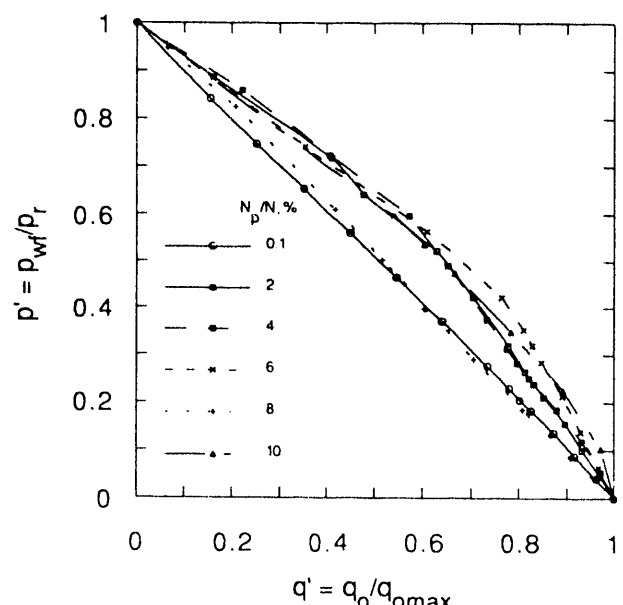


Fig. 29 75-Deg Slanted well inflow performance relationship; vertical permeability = 0.1 x horizontal permeability.

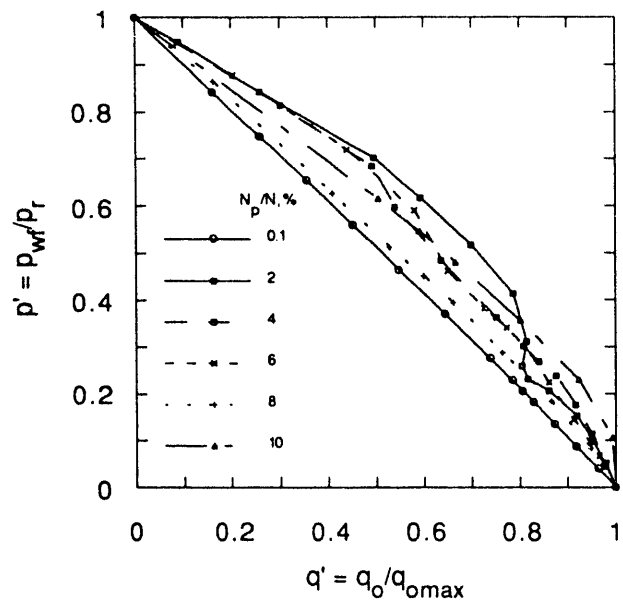


Fig. 30 75-Deg Slanted well inflow performance relationship; wellbore in bottom layer of  $19 \times 3 \times 3$  grid.

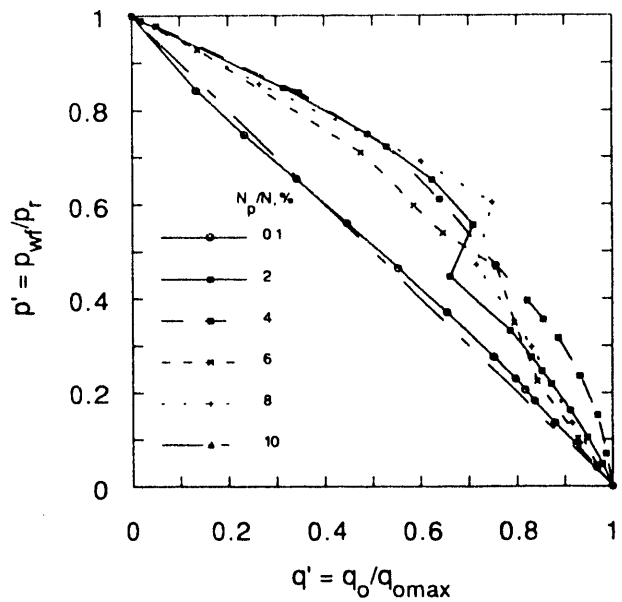


Fig. 32 75-Deg Slanted well inflow performance relationship; strata permeability = 40, 20, 10 mD (top, middle, and bottom).

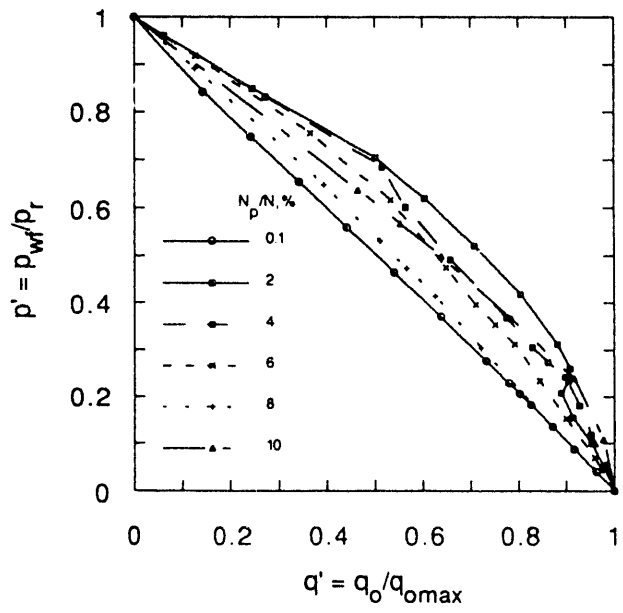


Fig. 31 75-Deg Slanted well inflow performance relationship; wellbore in top layer of  $19 \times 3 \times 3$  grid.

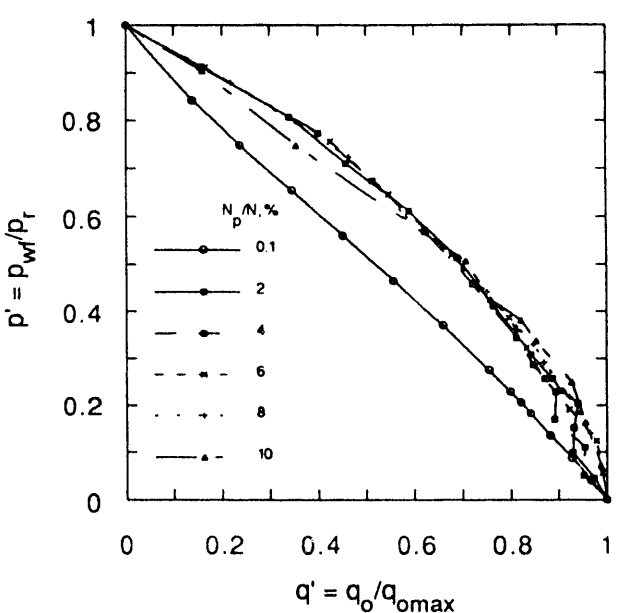


Fig. 33 75-Deg Slanted well inflow performance relationship; strata permeability = 10, 20, 40 mD (top, middle, and bottom).

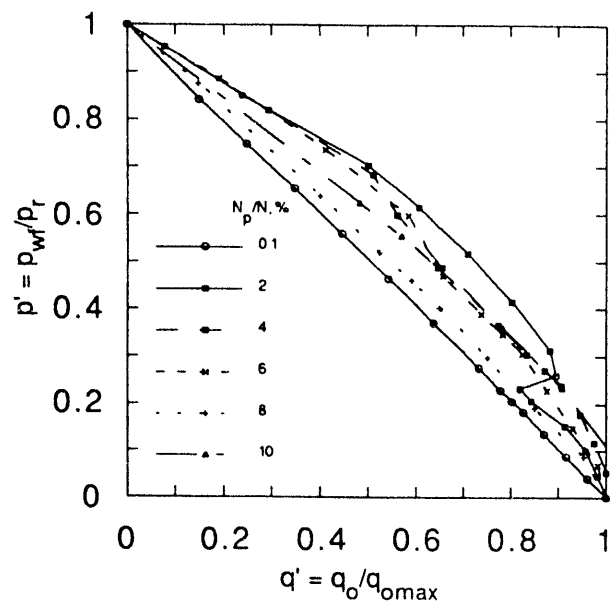


Fig. 34 75-Deg Slanted well inflow performance relationship; perforated length =  $1/3 \times$  total well length.

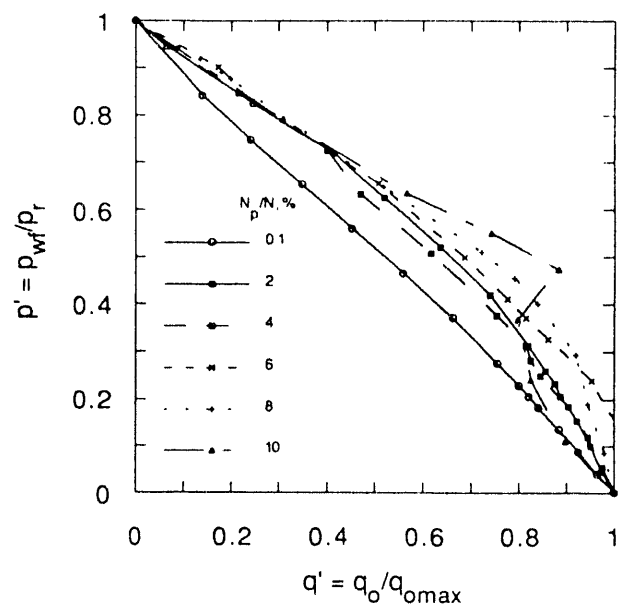


Fig. 36 75-Deg Slanted well inflow performance relationship; heterogeneous permeability, permeability decreases from left to right by 20%.

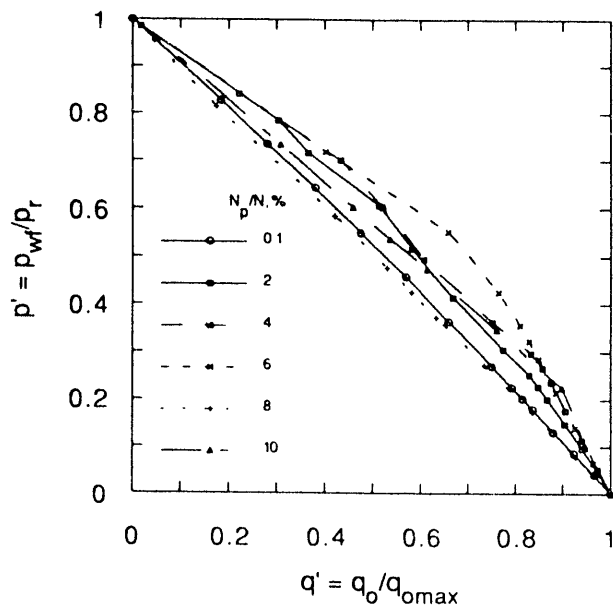


Fig. 35 75-Deg Slanted well inflow performance relationship; formation thickness = 235 ft = 10 x base case.

## APPENDIX A

### USER'S MANUAL FOR INFLOW PERFORMANCE RELATIONSHIP (IPR) GENERATOR

By Aaron M. Cheng, Raymond J. Heemstra, and James F. Pautz

## ABSTRACT

This manual provides user instructions for running the personal computer software IPR - an inflow performance relationship (IPR) generator. The main purpose of IPR is to interpolate the dimensionless inflow performance relationship results generated in SGP40 project.

## INTRODUCTION

For details of development of the IPR results used in this IPR software, refer to DOE report NIPER-573.<sup>1</sup> The IPR data generator uses a cubic spline fit to calculate a dimensionless flow rate ( $q'_i$ ) for a given dimensionless pressure ( $p'_i$ ) generated by natural cubic spline interpolation of inflow performance relationship (IPR) tables or curves derived from output files of the BOAST-VHS model. A normalized IPR curve is a plot of normalized flowing bottomhole pressure  $p'$  (y-axis) versus normalized oil flow rate  $q'$  (x-axis) at a given cumulative oil depletion, or oil recovery  $N_p/N$  in %, with  $p' = p_{wf}/p_r$  and  $q' = q_0/q_{0max}$ , where  $p_{wf}$  = flowing bottomhole pressure,  $p_r$  = average reservoir pressure,  $q_0$  = oil flow rate, and  $q_{0max}$  = maximum oil flow rate. The cumulative oil production  $N_p/N$  is selected from each table chosen from a built-in directory. The names of the tables in the directory include the following designated codes:

First two characters --

NH ----- horizontal well  
S1 ----- base case for slanted well with slant angle = 85.68 deg  
S2 ----- base case for slanted well with slant angle = 75.00 deg

Last one or two characters --

D ----- heterogeneous permeability  
E ----- wellbore in bottom layer  
E1 ----- wellbore in top layer  
H ----- base case  
H2 ----- formation thickness = 10 x base case  
K ----- vertical permeability = 0.1 x horizontal permeability  
L ----- perforated well length = 1/3 x total well length  
S ----- stratified system; strata permeability increases from top to bottom  
S1 ----- stratified system; strata permeability increases from bottom to top

## **System Requirements**

The minimum system requirements to run the IPR program on a microcomputer or personal computer are as follows:

Computer --- IBM PC, AT compatible, CPU may be 80286, 80386, or 80486.

Operating system --- PC - DOS, MS - DOS version 3.0 or later, or DRDOS 5.0.

Memory --- 512 K minimum, 640 K preferred (IPR program size is about 220K).

Disk capacity --- Application, IPR, will operate from the supplied 360K floppy drive, although a hard drive will be faster.

Math coprocessor --- 80287 math coprocessor. The program will not run without a math coprocessor.

Screen graphics --- Graphic plots are supported by the EGA, VGA, and super VGA color graphic adapter.

Graphic printer --- Screen graphics can be printed on an Epson/IBM compatible 9 pin dot matrix printer, including the IBM graphics printer and the Epson FX and MX series.

## **IPR Software and Related Files**

The 360K floppy disk supplied with this user's manual contains a total of 31 files. These are:

IPR.EXE --- Main application program.

Three supporting device drivers for the executable application code are developed by Heartland Software, Inc., 234 S. Franklin, Ames, Iowa 50010. These include:

DRAFT.FNT --- Default text font used for all the displayed graphical text.

SCREEN.CFG --- Default configuration screen device for the IBM color graphics card.

RASTER.CFG --- Default configuration raster device driver emulating an Epson/IBM compatible graphics printer.

The remaining 27 files are named as listed in the User's Instructions section. These are files created by using the inflow performance relationship (IPR) data generated by using the BOAST-VHS program as previously discussed.

## User Instructions for IPR

Under the DOS operating system, type in the name of the program, IPR, followed by a carriage return. An introduction screen is displayed which contains a short explanation of the program. The user is given a selection of tables to choose from in the form of a directory of data files. At this point, the user can request help on a description of the table names by optionally entering HELP, H, h, or help and then give the name of the data table name for which help is needed. If the user wishes to look over all the names, type in ALL or all. Appendix A explains the built-in file names for the IPR program. If help is not needed, the user merely types in the name of the file or table requested. Optionally, the user can enter the name of any external file name not listed in the directory, provided the same rules of format prevail in the file. These rules require tabs to separate the p's and q's in their respective columns. The IPR program is command driven, and the commands or prompts are very simple and self-explanatory. The example described in the next section shows a typical IPR run for interpolating  $q'_i$  for a given  $p'_i$ .

### Example of Running IPR

The following presents a typical example of the running IPR program. The user is assumed to have some knowledge of the DOS operating system. If the user is not familiar with DOS, he or she should refer to the MS-DOS or PC-DOS user's manual for the version used on your computers.

>IPR

### The Inflow Performance Relationship [IPR] data generator using BOAST-VHS output files

This program produces a dimensionless flow rate ( $q'_i$ ) for a given dimensionless pressure ( $p'_i$ ) generated by a cubic spline interpolation of tables of  $p'_i$  versus  $q'_i$  values derived from the BOAST-VHS model SGP40 project.<sup>1</sup> The cumulative oil depletion or recovery value (Np/N, %) is selected from each table chosen from a built-in directory. The names of the tables include the following designated codes:

NH - horizontal well	H - base case
S1 - slant angle of 85.68 deg.	E - bottom layer
S2 - slant angle of 75.00 deg.	E1 - top layer

H2 - h1 = 10h	K - Kv = 0.1*Kh
L - Lperf = 1/3 Lt	S & S1 - stratified systems.
The Inflow Performance Relationship	
data generator using BOASTVHS output files	

Do you wish a new input table? ( Y or N )  
(Type H for help or Q to quit ) : YES

(Enter a 0 for a new table)

NHH	NHD	NHE	NHE1	NHH2	NHK	NHL	NHS	NHS1
S1	S1D	S1E	S1E1	S1H2	S1K	S1L	S1S	S1S1
S2	S2D	S2E	S2E1	S2H2	S2K	S2L	S2S	S2S1

Enter input file name of new (p" versus. q") table.

(HELP or QUIT )

>HELP

Enter input table NAME for which help is needed (or ALL)

( or QUIT )

>S2S1

S2S1 - 75 deg-Slanted well;  
wellbore in top layer of 19 x 3 x 3 grid

Select a table from the following list.

(Enter a 0 for a new table)

NHH NHD NHE NHE1 NHH2 NHK NHL NHS NHS1  
S1 S1D S1E S1E1 S1H2 S1K S1L S1S S1S1  
S2 S2D S2E S2E1 S2H2 S2K S2L S2S S2S1

Enter input file name of new (p' versus q') table.

(HELP or QUIT )

>S2S1

Table ready for S2S1

(Enter a 0 for a new table)

<u>N</u>	<u>N<sub>p</sub>/N</u>
(1)	0.1
(2)	2.0
(3)	4.0
(4)	6.0
(5)	8.0
(6)	10.0

Choose N from 1 through 6 ( or -1 for all) : 6

A graph of the S2E1 file for N<sub>p</sub>/N = 10.0 % will be displayed on the computer screen.

Type -1 for all N<sub>p</sub>/N, 0 for new table, 1 to 6 for new N<sub>p</sub>/N,  
7 for printout of last graph, and >7 to restart.

Using N<sub>p</sub>/N = 10.0 from table S2E1

CHOOSE p' : .5

q' = 0.63781

Using N<sub>p</sub>/N = 10.0 from table S2E1

CHOOSE p' : .6

q' = 0.51325

Using N<sub>p</sub>/N = 10.0 from table S2E1

CHOOSE p' : 2

A graph of the S2E1 file for N<sub>p</sub>/N = 2.0 % will be displayed on the computer screen.

Type -1 for all N<sub>p</sub>/N, 0 for new table, 1 to 6 for new N<sub>p</sub>/N,  
7 for print out of last graph, and >7 to restart.

Using N<sub>p</sub>/N = 2.0 from table S2E1

CHOOSE p' : 0

(Enter a 0 for a new table)

NHH NHD NHE NHE1 NHH2 NHK NHL NHS NHS1  
S1 S1D S1E S1E1 S1H2 S1K S1L S1S S1S1  
S2 S2D S2E S2E1 S2H2 S2K S2L S2S S2S1

Enter input file name of new (p' versus. q') table.

(HELP or QUIT )

## ACKNOWLEDGMENTS

This project was conducted for the U. S. Department of Energy under Cooperative Agreement DE-FC22-83FE60149. Special thanks are due to Fred Burch and Thomas Reid of the DOE Bartlesville Project Office for their initiation and supervision of this project, and to Thomas E. Burchfield, Ming-Ming Chang, James F. Pautz, and Min Tham, all of NIPER, for their valuable ideas and technical support.

## REFERENCE

1. Cheng, A. M. Development of general Inflow Performance Relationships (IPR's) for Slanted and Horizontal Wells Producing Heterogeneous Solution-Gas Drive Reservoirs. DOE Report NIPER-573, November 1991.

## APPENDIX B

### DESCRIPTION OF IPR GENERATOR HELP COMMAND

>HELP

Enter input table NAME for which help is needed (or ALL)  
( or QUIT )

>ALL

HELP produces the whole of list of explanations if 'ALL' is selected or selects individual line of help based on the string 'WHICH' where a comparison is made between the user's selection and a list of table name files.

NHH - Horizontal well;  
base case using Vogel's base data (J. Pet. Tech., January, 1968, pp 83-92)  
NHD - Horizontal well;  
x-direction permeability decreases by 20 % from left to right  
NHE - Horizontal well;  
wellbore in bottom layer of 19 x 3 x 3 grid  
NHE1 - Horizontal well;  
wellbore in top layer of 19 x 3 x 3 grid  
NHH2 - Horizontal well;  
formation thickness = 235 ft = 10 x base case  
NHK - Horizontal well;  
vertical permeability = 2 md = 0.1 x base case  
NHL - Horizontal well;  
perforated length = 1/3 x total length  
NHS - Horizontal well;  
strata permeability = 40, 20, 10 md (top, middle, bottom)  
NHS1 - Horizontal well;  
strata permeability = 10, 20, 40 md (top, middle, bottom)

TYPE Carriage return to CONTINUE

S1 - 85.68 deg-Slanted well;  
base case using Vogel's base data (J. Pet. Tech., 1968)  
S1D - 85.68 deg-Slanted well;  
x-direction permeability decreases by 20 % from left to right  
S1E - 85.68 deg-Slanted well;  
wellbore in bottom layer of 19 x 3 x 3 grid  
S1E1 - 85.68 deg-Slanted well;  
wellbore in top layer of 19 x 3 x 3 grid  
S1H2 - 85.68 deg-Slanted well;  
formation thickness = 235 ft = 10 x base case  
S1K - 85.68 deg-Slanted well;  
vertical permeability = 2 mD = 0.1 x base case  
S1L - 85.68 deg-Slanted well;  
perforated length = 1/3 x total length  
S1S - 85.68 deg-Slanted well;  
strata permeability = 40, 20, 10 mD (top, middle, bottom)  
S1S1 - 85.68 deg-Slanted well;  
strata permeability = 10, 20, 40 mD (top, middle, bottom)

TYPE Carriage return to CONTINUE

S2 - 75 deg-Slanted well;  
base case using Vogel's base data (J. Pet. Tech., 1968)  
S2D - 75 deg-Slanted well;

x-direction permeability decreases by 20 % from left to right

S2E - 75 deg-Slanted well;

wellbore in bottom layer of 19 x 3 x 3 grid

S2E1 - 75 deg-Slanted well;

wellbore in top layer of 19 x 3 x 3 grid

S2H2 - 75 deg-Slanted well;

formation thickness = 235 ft = 10 x base case

S2K - 75 deg-Slanted well;

vertical permeability = 2 mD = 0.1 x base case

S2L - 75 deg- Slanted well;

perforated length = 1/3 x total length

S2S - 75 deg-Slanted well;

strata permeability = 40, 20, 10 mD (top, middle, bottom)

S2S1 - 75 deg-Slanted well;

strata permeability = 10, 20, 40 mD (top, middle, bottom)

(Enter a 0 for a new table)

NHH	NHD	NHE	NHE1	NHH2	NHK	NHL	NHS	NHS1
S1	S1D	S1E	S1E1	S1H2	S1K	S1L	S1S	S1S1
S2	S2D	S2E	S2E1	S2H2	S2K	S2L	S2S	S2S1

Enter input file name of new (p" versus q") table.

(HELP or QUIT )

>QUIT

END

DATE  
FILMED

6/12/92

